WELDING RESEARCH

SUPPLEMENT TO THE *WELDING JOURNAL*, AUGUST 1998
Sponsored by the American Welding Society and the Welding Research Council

Arc Initiation in Gas Metal Arc Welding

The integral of the square of the current is found to be a good indicator of arc start behavior and experiments and simulation show that arc starts are often improved by a fine-pointed wire tip

BY D. FARSON, C. CONRARDY, J. TALKINGTON, K. BAKER, T. KERSCHBAUMER AND P. EDWARDS

ABSTRACT. Arc initiation with gas metal arc welding (GMAW) was studied. Arc starts were observed experimentally using a high-speed video camera and computer data acquisition of arc current, voltage and wire feed speed waveforms. Tests were performed at short-circuiting and spray transfer machine settings and with clipped and unclipped wires.

The experimental data gathered during this work revealed that the initial melting of the wire extension occurred either at the base metal contact point or somewhere along the length of the extension. In the former cases, the arc tended to evolve smoothly to steady-state conditions. In the latter case, the arc either extinguished subsequent to initiation or was sustained and evolved to a steady-state condition. Extinguishment was more often observed at short-circuit conditions, while sustained arcs were more often observed under spray conditions. Initiation of the arc at the point of contact with the base metal was more likely to occur if the wire end was freshly clipped and/or if the wire feed speed was relatively low when contacting the base metal. However, this was not always the case. Thermal-electrical simulations of the wire extension during the early stages of arc initiation were performed. These simulations indicated that a finely pointed wire end should first melt at the point of contact with the base metal, while blunt wires should first melt at mid-extension. However, as noted above, the experimental results did not always conform to this prediction. A possible explanation for the differences between experimental and simulation results is unmodeled variations in wire-to-base metal contact resistance and geometry.

D. FARSON, K. BAKER, T. KERSCHBAUMER and P. EDWARDS are with Department of Industrial Welding and Systems Engineering, The Ohio State University, Columbus, Ohio. C. CONRARDY is with Welding Engineering Technologies, Hilliard, Ohio. J. TALKINGTON is with Edison Welding Institute, Columbus, Ohio.

Introduction

Reliable arc starting is particularly important for automated GMAW, where events occur in a preprogrammed, timed sequence. Delayed or intermittent arc starting can cause defects or unwelded regions at the beginning of the weld bead or more severe process malfunctions (*e.g.*, wire tangles or contact tube/wire fusion). In this work, a combined theoretical and experimental approach was taken to understand the initial phases of arc initiation in GMAW. The objectives were as follows:

1) Observe arc starts with a high-speed video system to record visually observable phenomena and with a computer data acquisition system to record the transient voltage, current and wire feed speed values.

2) Perform a coupled thermal-electrical simulation of the initial phases of arc initiation to assist in the interpretation of the experimental results.

3) Determine the effect of several basic process parameters on arc starting (including voltage and wire feed speed equipment settings and wire end condition) and the parameters most likely to result in quick, consistent arc initiation.

KEY WORDS

Arc Initiation
GMAW
Short Circuiting
Spray Transfer
Electrode Tip
Metal Transfer
Wire Heating
High-Speed Video

Background

The electrical heating and subsequent disintegration of metal wires have been the subjects of a considerable amount of research by the physics community. There are important applications in the design of conventional and nuclear ordinance and the subject contains some basic physics questions of fundamental interest in their own right. The state of the art of physical understanding in the late

1950s and early 1960s is summarized in a series of proceedings (Ref. 1). More recent work is reported in Refs. 2, 3. Although much of this work is pertinent to current densities much higher than is typical of arc welding, the physical analysis of the initial phases of conductor disintegration is directly applicable to the case of a GMAW arc start.

Table 1 — Welding Parameters

Voltage	22.2, 32 V
Wire feed speed	180, 300 in./min
Wire type	E70S-6
Wire diameter	0.045 in. (1.1 mm)
Contact tube-to-work distance	0.5 in. (12 mm)
Shielding gas	90 Ar - 10 CO_2
Travel speed	20 in./min (0.51 m/min)
Base material	A36, surface ground

The events occurring in the early phases of the disintegration of an electrically heated wire are dominated by resistive heating. The generation of heat (Joule heating) at any given location in this circuit is directly dependent on the resistance at that point and the current flow (which is, of course, the same at all points along the circuit).

$$Q(t) = \int_{\tau=0}^{t} i^2(\tau)R(\tau)d\tau \quad (1)$$

where Q(t) is the total amount of electrically generated energy in a section of wire from the time that current starts to flow (t = 0), R(τ) is the time-varying resistance of the wire segment under consideration and i(t) is the time-varying current. The resistance of the wire segment is a function of its length, cross-sectional area and material resistivity, which is generally an increasing function of temperature for metals.

$$R(T) = \rho_e \, l/A \quad (2)$$

where l = length, A = cross-sectional area and ρ_e = electrical resistivity. In this work, the resistivity of steel was assumed to increase linearly with temperature at a constant rate

$$\rho_e(T) = \rho_e(T_o) + \frac{d\rho_e(T)}{dT}\Big|_{T_o}(T \pm T_o) \quad (3)$$

The enthalpy of the wire segment is directly related to Joule heat generation and is the parameter that determines the state (whether solid, liquid or vapor) of the material. For this reason, it is common to correlate experimentally observed "exploding wire" events to an expression commonly called the action integral, g(t), and defined (for the simple case of a material with fixed composition and size) by the integral (Ref. 1).

$$g(t) = \int_{\tau=0}^{t} i^2(\tau)d\tau \quad (4)$$

The generation of heat in the weld wire is balanced by energy losses to the surroundings and energy storage in the material, resulting in temperature increases in the latter. These processes are described by an energy balance differential equation (the "heat equation"[Ref. 4])

$$\rho c(T)\frac{\partial T(r,t)}{\partial t} = \nabla \cdot \left[k(t)\nabla T(r,t)\right] + q_e(r,t) \quad (5)$$

where ρ is density, c is the specific heat, T is the temperature in the material, k is the thermal conductivity, ∇ is the vector derivative operator, q_e is the rate of volumetric heat generation and r and t are space and time variables. Boundary conditions such as $T(r_w,t) = T_w$ (fixed boundary temperature at a wall), $k(\partial T/\partial n) = h(T_w - T_a)$ (a convective boundary condition where n is a boundary normal direction, h is a convection coefficient, T_w is a boundary temperature and T_a is ambient temperature) and initial conditions such as $T(r,0) = T_0$ are needed to solve the heat equation.

The rate of volumetric heat generation is determined by the current flow in the material as discussed above. However, evaluation of the heat generation in a conductor of varying cross-sectional area and temperature distribution requires detailed knowledge of current flow distribution in the material. The potential (voltage) field V in a current-conducting material with temperature-varying resistivity satisfies a general form of Laplace's equation (Ref. 5)

Table 2 — Experimental Conditions and Results

Weld No.	Wire Speed Set in./min (m/min)	Volt Set	Wire Clipped 1 = Y, 0 = N	Wire Speed @ Short	Action
4	180 (4.6)	22	1	160	3.04E + 02
7	180 (4.6)	22	0	123	1.14E + 04
8	180 (4.6)	22	1	163	1.21E + 04
9	180 (4.6)	22	1	213	2.11E + 03
10	180 (4.6)	22	1	166	1.18E + 04
11	180 (4.6)	22	0	8	2.06E + 01
12	180 (4.6)	22	0	141	1.21E + 02
13	180 (4.6)	22	0	166	6.58E + 02
14	180 (4.6)	22	1	151	1.13E + 04
15	180 (4.6)	22	1	121	9.00E + 01
16	180 (4.6)	22	0	150	1.09E + 04
17	180 (4.6)	22	1	193	1.16E + 04
18	300 (7.6)	32	0	148	1.11E + 04
19	300 (7.6)	32	0	298	1.16E + 04
20	300 (7.6)	32	0	301	1.18E + 04
21	300 (7.6)	32	1	133	8.04E + 00
22	300 (7.6)	32	1	184	1.14E + 04
24	300 (7.6)	32	1	186	1.15E + 04
29	300 (7.6)	32	1	159	1.14E + 04
30	300 (7.6)	32	1	234	1.16E + 04
31	300 (7.6)	32	0	228	1.10E + 04
32	300 (7.6)	32	0	274	7.60E + 02
33	300 (7.6)	32	1	147	2.14E + 01
36	300 (7.6)	32	1	205	1.10E + 04

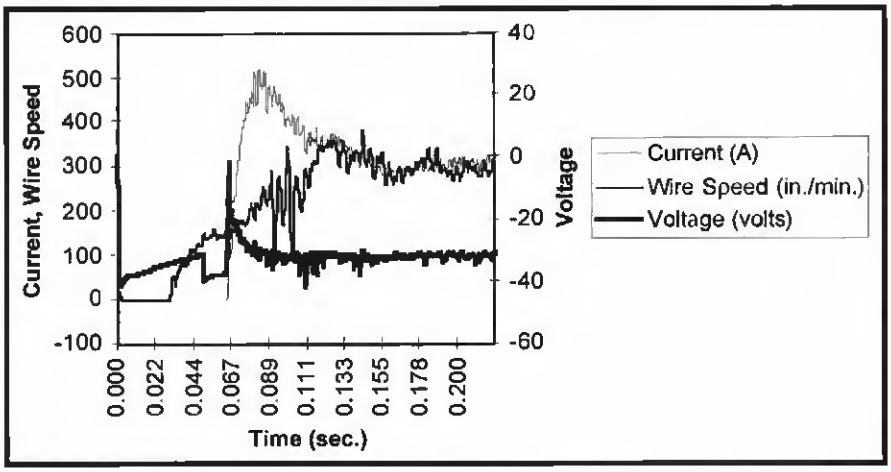

Fig. 1 — Plot of current, wire feed speed and voltage waveforms for Weld No. 33 where a smooth arc start and subsequent spray transfer was observed.

$$\nabla \cdot \frac{1}{\rho_e(T)} \nabla V = 0 \quad (6)$$

and current and voltage are related by the vector equivalent of Ohm's Law (Ref. 6)

$$\rho_e J = \frac{\partial V}{\partial r} \quad (7)$$

where J is current density (amp m^{-2}). Solution of Laplace's equation yields the scalar potential field in the material, from which the current density and subsequent Joule heating, q_e, can be derived. The solution requires boundary condition specifications such as $V(r_w, t) = V_w$ (a fixed boundary voltage) and Ohm's law for current flow normal to a boundary

$$J_n = \frac{1}{\rho_e} \frac{\partial V}{\partial n}\Big|_{r_w} \quad (8)$$

where J_n is current density normal to a boundary located at r_w. Finally, note that since Joule heating appears as a source term, the heat equation is coupled with Laplace's equation (which involves temperature-dependent resistivity) and the two must be solved simultaneously, generally by iteration.

It must be noted that the heating phenomena described above are of primary importance in the early (and most time-consuming) phase of wire disintegration. Following melting, magnetic pinch forces rapidly reduce the cross-sectional area of the conductor (Ref. 7), joule heating rapidly increases and expulsion of the melt results. At this point, current conduction is maintained by an arc that grows in length as the wire disintegration process evolves to completion.

There is some prior literature dealing with arc starting in the GMAW process. Melton (Ref. 8) briefly describes the application of the action integral to the analysis of the initial phases of GMAW arc starting and mentions the importance of a sharply pointed tip in rapid arc initiation. Dilthey (Ref. 9) describes a special wire feeder that performs a touch-retract function to reliably start the GMA welding arc. Manz also describes the application of a "sensitivity integral" to the prediction of arc starting times (Ref. 10). Finally, Lenivkin (Ref. 11) reports some experimental current/voltage measurements in the case of arc starting and describes a simple, one-dimensional simulation to represent the initial phases of the arc initiation process.

Experimental Procedure

A Hobart MegaPulse 450 power source/wire feeding system was used to conduct a series of arc starting experiments. The power supply was operated in constant voltage (*i.e.*, nonpulsed) mode. The welding conditions are summarized in Table 1. Arc starts were made with a matrix of voltage and wire feed speed settings and wire conditions (the end of the wire was either in a freshly clipped state or unclipped and balled from the previous weld). The arc current and voltage were sampled at a 4500-Hz rate using a computer data acquisition system. The arc voltage was measured between the contact tube and workpiece and the arc current was measured with a shunt resistor in series with the welding gun lead. The wire feed speed was monitored by sampling the voltage output of a tachometer in contact with the wire near the motor end of the torch liner. High-speed video images of the arc starts were taken using a Kodak EktraPro 4540 high-speed camera operating at a rate of 4500 frames per second. A 15-W copper vapor laser strobe was used to enhance image quality, allowing clear visualization of the arc start phenomena. The power supply contactor, wire feed motor and welding gun travel motor were all started simultaneously at the beginning of each weld run. Since a delay time was required for the wire to actually contact the base metal, the travel axis was moving at the time of wire contact.

Experimental Results

The experimental matrix of wire feed speed, voltage and wire condition is shown in Table 2. Also included in this table are the actual wire feed speed (measured at the time the wire first contacted the base metal) and the value of the action integral for the initial breakdown of the wire. The voltage and wire feed settings used in these tests correspond to short-circuiting transfer (weld no. 4 –17) and spray transfer (weld no. 18 –33). The action integral was calculated by Euler integration of the square of the time samples of the weld current. Only that portion of the current waveform corresponding to the first "explosion" of the wire extension was included in the integral. The beginning of the integration interval was identified as the first nonzero current value. The end of the integration interval was identified as the point where the voltage rapidly increased from short circuit value (typically about 10–12 V) to a larger value. The length of the integration interval was typically 20 ms but was sometimes much lower. This integration included the rise time of the current, which typically took about 10 ms to reach a maximum value. This value would be expected to vary with different power supplies, as would other transient characteristics, such as current fall time during arc extinguishments.

Measured current, voltage and wire feed speed waveforms corresponding to Weld No. 33 (where spray transfer settings were used) are shown in Fig. 1. The data indicates a smooth arc start and transition to spray transfer. The current abruptly increased (and voltage decreased) at short circuit and then settled back to the steady state value over a time of about 30 ms. The arc initiation is visible early in the current upslope at a point where the voltage magnitude abruptly increased from near 0 to near 20 V. From Table 2, the action integral of this arc start was relatively low, only about 2.14×10^1.

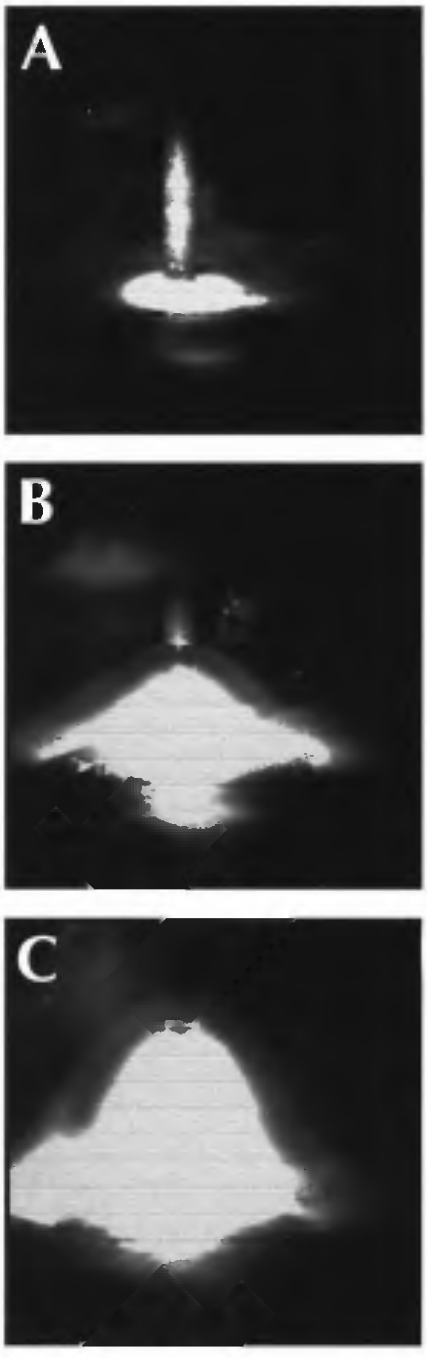

Fig. 2 — Sequence of images corresponding to Weld No. 33.

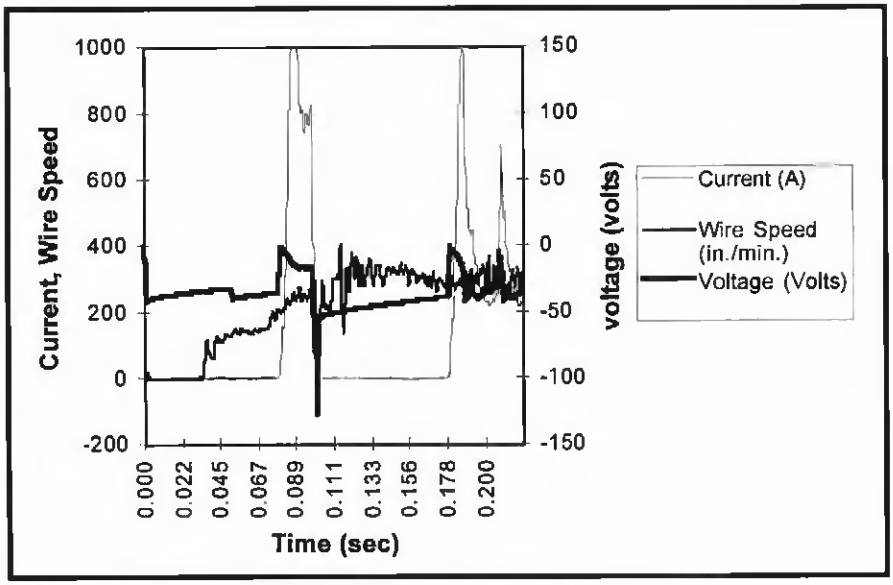

Fig. 3 — Plot of current, wire feed speed and voltage waveforms for Weld No. 36 where the entire wire extension disintegrated and the arc extinguished.

The wire feed speed waveform reveals relatively large oscillations in the wire velocity shortly after arc initiation. This was observed to some extent in almost all of the tests. Evidently, the high force associated with the wire "stubbing" on the workpiece and the sudden release of this force during arc initiation perturbed the wire feed system significantly and smooth feeding was not maintained for a time after the arc initiation. It should be emphasized that wire speed was measured at the feed motor and not at the contact tube. Thus, the actual motion of the wire as it feeds from the welding gun may not correspond exactly to the speed measurements taken at the feeder. However, it is interesting to note that the current and wire feed speed waveforms oscillate in unison during this transient period, as would be expected if the speed of the wire feed exiting from the welding gun were oscillating. Furthermore, oscillation in the speed of the wire extension was also evident in the high-speed video images of the arc starts.

In Fig. 2, a sequence of high-speed video images of this arc start are displayed. The first image in Fig. 2A corresponds to a time very shortly after arc initiation (near sample number 320 in Fig. 1). Note that the arc initiated by fusion of the wire at the point of contact with the base metal. The second and third images correspond to times in the initial upslope of the current (near sample numbers 325 and 350, respectively). They show that the arc length smoothly increased to a steady-state value.

Measured current, voltage and wire feed speed waveforms corresponding to Weld No. 36 (where spray transfer settings were used) are shown in Fig. 3. The arc start indicated by this data is much more violent than that of the previous data set. The current quickly ramps up to the maximum transient short-circuit capacity of the system (near 1000 A) and it remained near this high level for about 20 ms. After the arc initiation (near sample No. 440), the current dropped back to 0 A, indicating that the arc extinguished. The voltage likewise returned to the open circuit value. After a long period with no events, the arc reinitiated and then was sustained. The action integral associated with the first arc initiation was relatively high, about 1.1×10^4.

A video sequence corresponding to the first arc initiation of Weld No. 36 is shown in Fig. 4. Figure 4A shows the period after short circuit but prior to arc initiation when the high current levels heated the wire. Smoke from some antispatter compound used in conjunction with this particular test evolved from the heated wire and is visible in the image. The next image in Fig. 4B corresponds to sample number 444 where the voltage magnitude first increased from short circuit. The picture reveals that this event is associated with breakdown of the wire column at a point near the contact tip. Figure 4C shows the rapid destruction of the wire several tenths of a millisecond later. Note that a long portion of unvaporized wire visible in the image is noticeably curved, suggesting that it was at or near the melting temperature at this point in time.

Measured current, voltage and wire feed speed waveforms corresponding to Weld No. 18 (where spray transfer settings were used) are shown in Fig. 5. The data show an arc initiation quite similar to Weld No. 36 at its beginning. The main difference from the prior example is that the arc was sustained after initiation and a smooth transition to spray transfer ensued. Video images of this arc start (which are not shown) revealed that initial disintegration of the wire extension occurred near the midpoint, very similar to those of Fig. 4. The similarity of the action integral value for this start (1.11×10^4) to that of Weld No. 36 should also be noted.

Further analysis of the experimental data (including images and waveforms that are not included here due to space limitations) reveals that most of the arc starts were approximately similar to one of the three previous examples. In the following weld tests, the wire extension disintegrated somewhere other than the base metal contact point and subsequently extinguished: 6, 7, 10, 12, 17, 36. In other cases, the wire disintegrated at other than the base metal contact point but was sustained afterward: 16, 18, 19, 20, 22, 24, 25, 28, 29, 30, 31. Finally, in some tests, the wire extension disintegrated at the base metal contact point and smoothly evolved to its steady state condition: 4, 9, 11, 12, 13, 15, 21, 24, 32, 33.

This study reveals that some generalizations may be drawn from these results. First, it is evident that the high-voltage spray transfer settings were much more likely to result in sustenance of the arc no matter how smoothly it initiated. All but one of the cases where the arc extinguished were tests with short-circuiting parameters.

The value of the action integral was a very good indicator of the disintegration mode of the wire extension. In all cases where the wire disintegrated somewhere in its middle section, the action integral was consistently high. Statistical analysis of these cases revealed that the mean of the action integral was 11,500 and the standard deviation was only 336. On the other hand, those cases where the wire disintegrated at the base metal contact had lower action integral values, but the variation was higher (values ranged from 20.6 to 2110). The arc starts displaying lower action integral appeared preferable as they generally were followed by smooth evolution of the arc to steady-state conditions. At short-circuit settings, a high action value start was likely to result in subsequent arc extinguishment, delaying the time until uniform short circuiting was achieved. Such behavior would tend to cause unwelded areas at the beginning of a weld. At spray settings,

high action value starts tended to be sustained, but in some videos, arcing to the contact tube was evident. Presumably, such behavior would promote fusion of the wire to the tube and/or high tube deterioration rates.

Unfortunately, the arc data does not provide clear guidance on how to obtain the smoother starts corresponding to lower action values. Analysis of the data reveals that the lower action integral values were somewhat more likely to be obtained at short circuiting conditions and when the wire was clipped. However, the correlation is not perfect. A number of low action value starts were obtained with no wire clipping and at spray transfer settings. Explanations for this random behavior may lie with inconsistencies in the base metal surface condition (in some cases, arc starts were made at the end of previous passes) or with inconsistency in the shape of the wire end in the unclipped state. In some cases, a large ball was observed on the unclipped wire end while in other cases, the end appeared sharper.

Simulation

To better understand the effects of the shape of the wire tip on arc initiation, physical phenomena occurring in the unfused wire extension during the first phase of arc initiation was simulated. The primary goal of this work was to identify the portion of the wire extension that would first become molten (and hence, fuse and initiate an arc). Evidently, if this occurs at the contact with the base metal, then an arc will initiate at the tip of the wire and a stable arc start may result. If melting first occurs in the middle of the wire extension, then the arc will establish there, which is a less desirable event.

A thermal-electrical simulation of the wire extension was carried out, requiring simultaneous solution of the Laplace and heat equations discussed earlier. Cross sections of the circular geometry and boundary conditions of two simulation cases are depicted in Figs. 6 and 7. In the first case, the wire tip was assumed to be blunt and in good thermal and electrical contact with the base metal. Hence, the lower tip of the wire was assumed to remain at room temperature and at ground potential (0 V) during the arc initiation event. The upper end of the wire extension was assumed to be in good thermal and electrical contact with the contact tube. Thus, the temperature of the upper end of the extension was assumed to remain at room temperature and a total current flow of 1000 A was uniformly distributed over the cylindrical wire cross-section. The second case was identical except the wire was assumed to have a sharp tip, as depicted. Thermo-physical parameters used in the simulation (corresponding to low-carbon steel) are given in Table 3. The primary simulation output was the temperature distribution in the wire at a specified time after the start of current flow (assumed constant at 1000 A). The simulation was performed using a commercially available finite element code (Ref. 12)

Table 3 — Thermophysical Parameters of Steel for Simulation

Heat Capacity ($J\ kg^{-1}\ C^{-1}$)	750
Thermal Conductivity ($J\ s^{-1}\ m^{-1}\ K^{-1}$)	50
Density ($kg\ m^{-3}$)	7900
Electrical Resistivity (ohm m)	$15 \times 10^{-8} + 0.004 \times 10^{-8} \cdot T$ (C)

A comparison of the simulated temperature fields for two of the cases is shown in Figs. 8 and 9. In both cases, only the tip of the wire is shown so that more details can be resolved. The simulation results show that the temperature distribution in the two wire segments was dramatically different. In the case of the tapered wire, the maximum temperature is achieved in a region very near the tip. At the same point in time, the temperature of the upper section of the wire was still very near to room temperature. This indicates that disintegration of a wire having this shape would first occur near the base metal. On the other hand, the blunt wire achieved melting temperature in a very broad region near the middle of the extension length. Due to effective cooling by conduction to the base metal, the lower end of the wire remained near room temperature. This indicates that a wire having this geometry would first disintegrate over a large region near the center of the extension.

The time taken for the maximum temperature in the simulated wire to reach the melting temperature is also near that observed experimentally. For the cases where the entire wire extension disintegrated, the time taken was typically about 20 ms from the time current first began to flow. In the simulation, the time for the extension to reach melting was about 10 ms. The longer experimental value is explained by the fact that the high short-circuit current levels were not reached instantly; the maximum current levels were typically achieved in about 10 ms — Fig. 3. Also, the wire presumably would disintegrate some time after the instant in which melting is first reached. The sharply tapered wire melted after about 0.1 ms in the simulation. Experimentally, the time taken for the wire to fuse was about 2 ms, somewhat longer than the simulation value.

Fig. 4 — Sequence of images corresponding to Weld No. 36.

In some cases, the predicted and observed disintegration modes were well matched, but there was "scatter" in this correlation. A number of blunt wires (those having a ball on the end from the previous weld) were observed to disintegrate first at midextension and a number of freshly clipped wires were observed to disintegrate first at the tip. However, quite a number of freshly clipped wires were also observed to disintegrate at midsection and a few unclipped wires

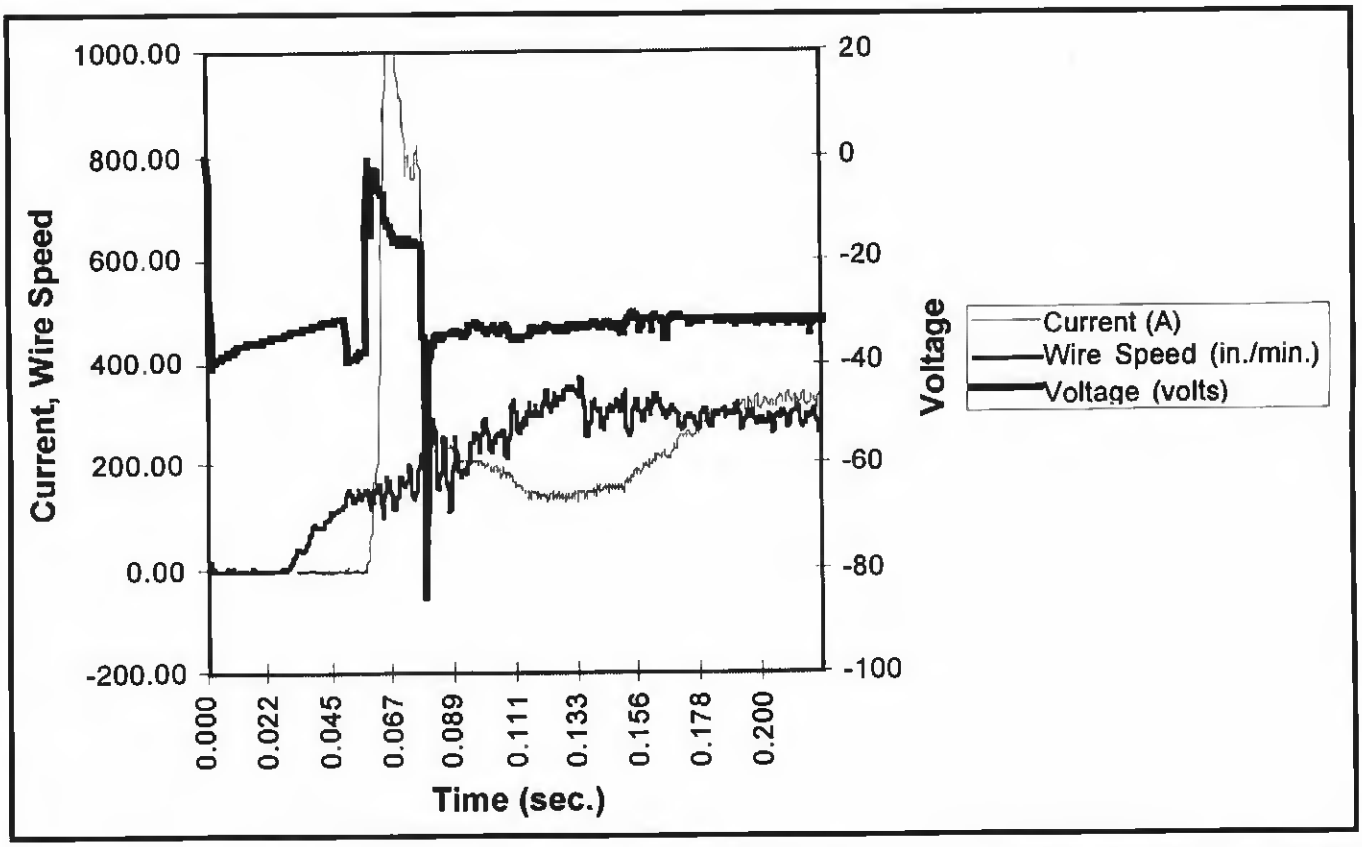

Fig. 5 — Plot of Weld No. 18 current, wire feed speed and voltage waveforms for a case where a violent arc start and subsequent spray transfer were observed.

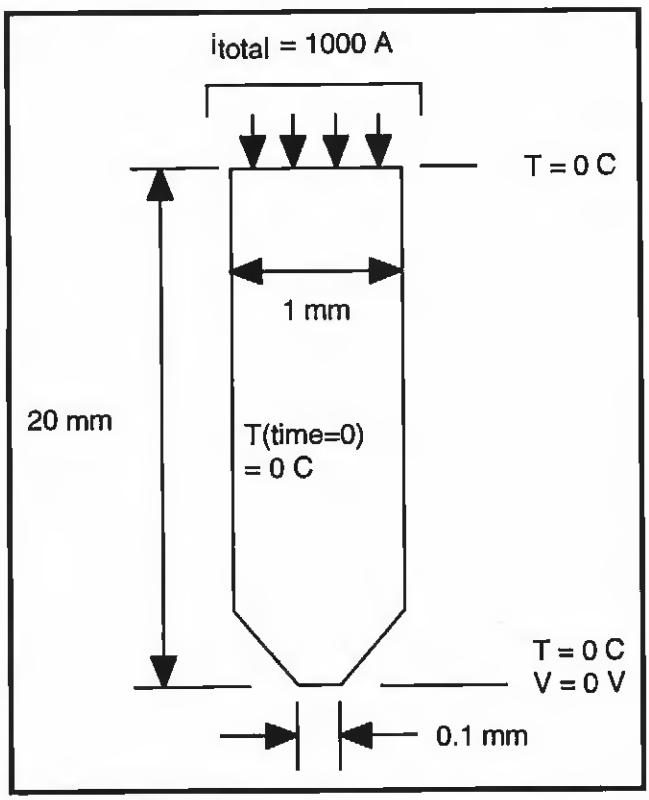

Fig. 6 — Geometry, boundary and initial conditions for tapered wire simulation.

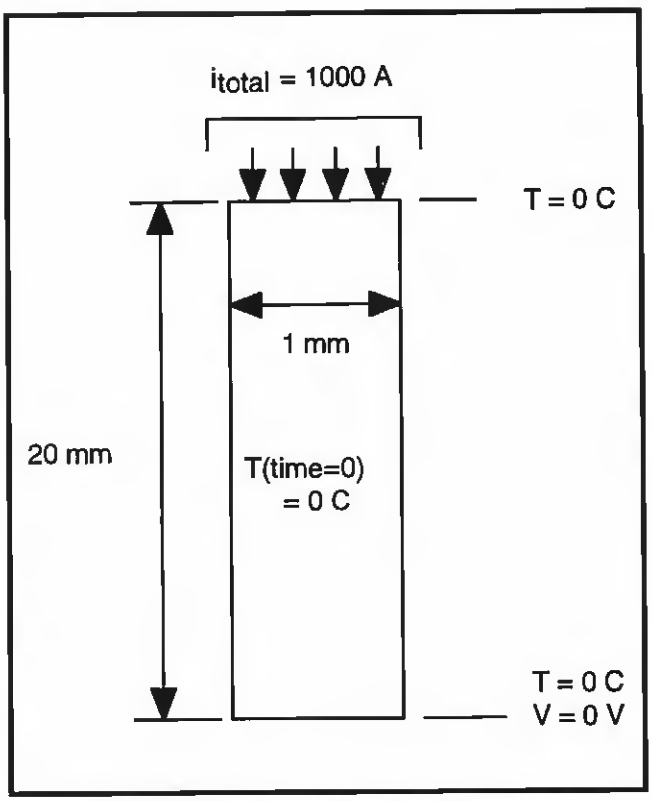

Fig. 7 — Geometry, boundary and initial conditions for blunt wire simulation.

were observed to disintegrate at the base metal contact point. The latter cases can likely be explained by uneven electrical contact between the wire and the base material. In such a case, where only a small portion of the blunt end achieves good thermal and electrical contact, the current flow would be highly concentrated (just as if the wire were tapered) and disintegration would likely occur at the tip. The cases of pointed wires disintegrating at midsection might be explained by the wire contacting at a broader area than is assumed in the simulations. The wire cutters used in the experiments did not always produce a finely pointed wire. Furthermore, the wire end tapered only in one direction. If the cutting tool happened to be perpendicular to the wire axis during clipping, a wire end that could conceivably have a relatively broad contact with the base material would result. Such uncontrolled variations could explain both the statistical nature of the experimental results and the differences between the simulations and experiments. The effect of a less-blunt wire tip on the initial temperature field is illustrated in Fig. 10. The simulated geometry has a tip diameter of 0.5 mm, half that of the nominal wire diameter. Note that the area that first melted in the simulation (which was achieved in 9 ms) was much further up the taper near the straight portion of the wire. Based on the time to melt, the action integral of this wire fusion event would be nearly equal to that of the case of the blunt wire.

Conclusions

The experimental data gathered during this work revealed basically two modes of GMAW arc initiation. In one, the initial disintegration of the wire extension occurred at the base metal contact point. In these cases, the arc tended to evolve smoothly to steady-state conditions and the action integral associated with the arc initiation was low. In another initiation mode, the wire disintegrated at mid extension. In these cases, the arc either extinguished subsequent to initiation or was sustained and evolved to a steady-state condition and the action integral was consistently high. The former was more often observed at short-circuit conditions while the latter was observed under spray conditions.

Initiation of the arc at the point of contact with the base metal was somewhat more likely to occur if the wire end was freshly clipped and/or if the wire feed speed was relatively low when contacting the base metal.

Simulations revealed that a finely pointed wire end was much more likely to disintegrate near the point of contact with the base metal than a blunt wire. However, as noted above, the experimental results did not always conform to this prediction.

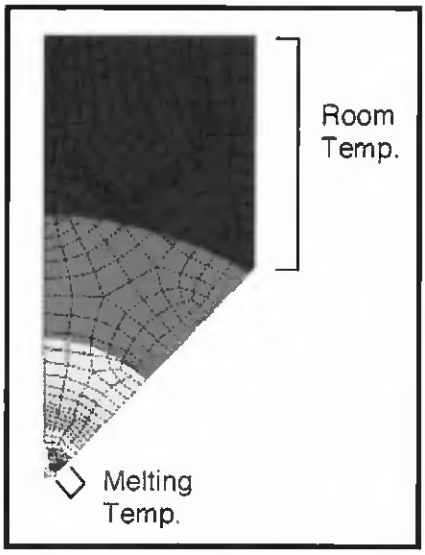

Fig. 8 — Simulated temperature field for a tapered wire tip.

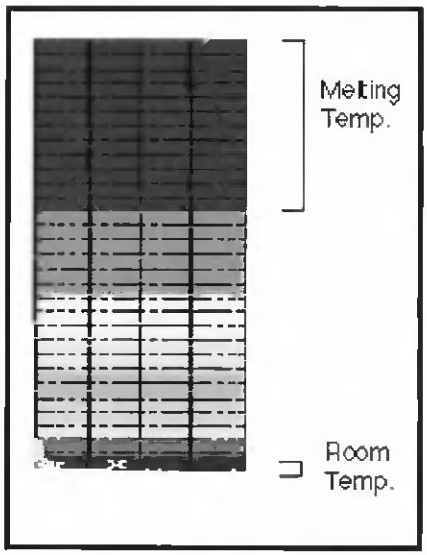

Fig. 9 — Simulated temperature field for a blunt wire tip.

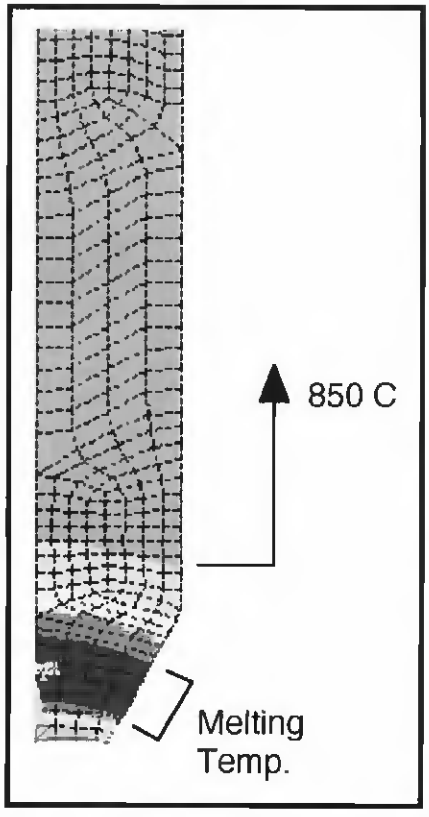

Fig. 10 — Simulated temperature field for a moderately tapered wire tip.

References

1. *Exploding Wires*, Vol. 1–4, 1959. Ed. W. G. Chace and H. K. Moore, Plenum Press, N.Y.

2. Linemuth, I. R., Brownell, J. H., Greene, A. E., Nickel, G. H., Oliphant, T. A., and Weiss, D. L. 1985. A computational model of exploding metallic fuses for multimegajoule switching. *Jour. Applied Physics*, 57: 4447.

3. Me-Bar, Y., and Harel, R. 1995. *Jour. Applied Physics*, 79, p. 1864.

4. Kuo, S. 1996. *Transport Phenomena and Materials Processing*, J Wiley & Sons, N.Y., p. 141.

5. Kraus, J. D., and Carver, K. R. 1973. *Electromagnetics*, 2nd ed., McGraw-Hill, N.Y. p. 133.

6. *Ibid.*, p. 118.

7. Lancaster, J. F. 1986. *The Physics of Welding*, 2nd ed., Pergamon Press, Oxford, England, pp. 237–244.

8. Melton, G. B. 1987. Factors affecting MIG arc initiation in mechanized systems. *The Welding Institute Research Bulletin*, The Welding Institute, Cambridge, England, July, p. 229–230.

9. Dilthey, U., Eichhorn, F., Groten, G., and Matzner, H. 1990. Spatter free ignition of the arc in GMA welding. *Proceedings Welding and Cutting '90 Conference*, Garmisch-Partenkirchen, pp. 27–31, Sept.

10. Manz, A. F. 1963. Predicting consumable electrode arc start times by the sensitivity integral. Welding Journal 42(9): 430–439.

11. Lenivkin, V. A. 1982. Initiation of the arc welding process with a consumable electrode. *Svar. Proiz.*, no. 8, pp. 9–11.

12. computer code Ansys, 1996. University Ver., Ansys, Inc., Canonsburg, Pa.